High-throughput deconvolution-resolved computational spectrometer

Jiang Yue (岳 江), Jing Han (韩 静), Yi Zhang (张 毅), and Lianfa Bai (柏连发)*

School of Electronic Engineering and Optoelectronic Technology, Nanjing University of Science and Technology, Nanjing 210094, China

**Corresponding author: mrblf@163.com*

Received November 28, 2013; accepted March 5, 2014; posted online April 4, 2014

A novel high-throughput spectrometer with a wide-slit is presented. In conventional spectrometers, the slit limited the light throughput. Here, the slit is replaced with a much wider one (200 μm) to increase throughput. A beam splitter is utilized to construct a dual-path optics to measure both non-dispersed and dispersed light intensity which comes from the wide-slit. While the dispersed light intensity is result of the non-dispersed light convoluted spectrum of the source, the spectrum can be acquired by solving the inverse problem of deconvolution. Experiments show that the reconstructed spectra achieved almost the same resolution measured by traditional spectrometer, while throughput and peak signal-to-noise ratio (PSNR) are improved dramatically.

OCIS codes: 300.6190, 100.6640, 100.3190.
doi: 10.3788/COL201412.043001.

High-throughput and high spectral resolution are essential demands for spectrometers. Conventional slit-based spectrometer requires the input slit should be narrow to achieve a reasonable resolution, due to too small slit cannot gather enough radiation. A number of designs have been presented to address the demands. Also a method could maximize the throughput without sacrificing spectral resolution, we call it having the Jacquinot advantage[1].

Over past several decades, two most important approaches were proposed to improve the performance of spectrometer. One is coded aperture spectrometer (CAS) and the other is Fourier transform spectrometer (FTS). CAS replaces the slit with a two dimensional coded matrix aperture, which is called a mask. And it was introduced as a multi-slit spectrometer to increase light throughput without loss of spectral resolution[2]. After more than half century development, the major CAS is Hadamard- transform spectrometers (HTS)[3,4]. Most encoded aperture theories are based on Hadamard matrices now. However, in recent years some new static, multiplex CASs were proposed based on new mathematical models[2,5]. For a CAS, a better spectral resolution lays on smaller mask features. Unfortunately, diffraction and optical blur negate the advantages for the small mask feature[6]. Apart from CAS, FTS is another method exhibiting Jacquinot advantage, it records interference patterns to estimate the spectrum of the incident light. But a classic FTS usually containing mechanical scanning elements prevents itself to be assembled easily, compactly and cheaply. Hence, attempting on eliminating moving parts to make a smaller, more reliable and inexpensive system is studied in recent years[7−9].

The key component of CAS is that it measures weighted multiple spectral channels instead of a single one for improving throughput and signal-to-noise ratio (SNR). However, there were several critical drawbacks caused by coded aperture. First of all, high precision and high resolution coded aperture is not available now. Then, the system needs small mask feature to achieve high spectral resolution, but it will bring unexpected diffraction and optical blur. In this letter, a novel high-throughput, spectral-channel-multiplied spectrometer without a spatial filter is presented, wherein spectrum is reconstructed by solving an inverse problem of deconvolution. The new design will achieve higher resolution or longer spectral range without bringing any aberration in by eliminating physical spatial modulator such as a coded aperture. Furthermore, the proposed system is stationary without any moving parts; and it is not much sensitive to shake compared with FTS. Figure 1 shows a schematic of the deconvolution-resolved computational spectrometer (DSCS).

In Fig. 1, there are two optical paths, both non-dispersed and dispersed light intensity can be measured. One path is based on a typical slit-based spectrometer, which it is indicated as dispersed-branch. The other path is called non-dispersed-branch. Based on this structure, lights intensity measured by CCD 2nd is the result of light intensity measured by CCD 1st convoluted spectrum of the light source. This relation is demonstrated in following paragraphs.

The detail about the system is described as follows. Light of the source is focused on a wide-slit (width of 200 μm) by objective lens (focal length (FL): 50 mm,

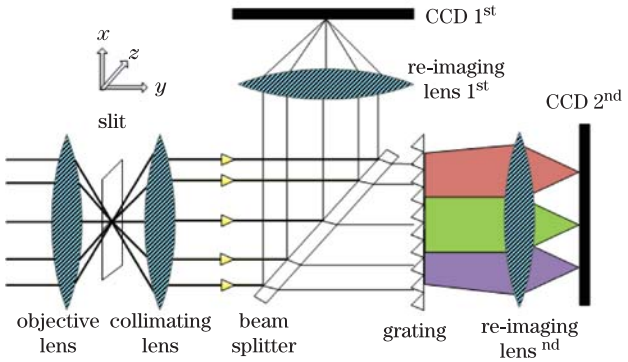

Fig. 1. (Color online) Schematic of the DSCS system.

 © 2014 Chinese Optics Letters

f-number: 1.4). The image plane of collimating lens is also fixed on the slit to make sure that the light passed though would be collimated light. Then the light beam is split into two by the beam-splitter. Considering that light is projected on much more pixels of CCD 2nd in dispersed-branch, unequal splitting (30% reflection, 70% transmission) tries to make SNR of the two branches equal. After that, the reflected light is refocused on CCD 1st by the re-imaging 1st lens. According to the reversibility principle of optical path, the image on the slit would be the same as image on the CCD 1st. In the dispersed-branch, the transmitted light irradiates on the grating vertically, and dispersed following the grating equation:

$$d(\sin\theta_i \pm \sin\theta) = j\lambda, \tag{1}$$

where θ_i is the incident angle and θ is the diffraction angel. If the slit is more than one pixel along x-axis, which is the direction spectrum dispersed, it causes overlapping of different wavelengths from adjacent pixels. This phenomenon is described in Fig. 2 in a brief way.

Figure 2 shows an ideal physical mechanism. Images on the two CCDs obey one rule: if a pixel on the slit is shifted L pixels along x-axis, the related non-dispersed pixel on CCD 1st and dispersed pixels on CCD 2nd would shift the same distance and direction, which it is called shift invariability. A brief derivation is presented as follows. Two pixels on the slit along the x-axis are taken as an example. Lights from the two pixels are turned into two beams of collimated light individually. The two beams of light have different incident angles, θ_{i1} and θ_{i2} before traveling into the grating. According to Eq. (1), diffraction angels related to different incident angles, θ_{i1} and θ_{i2} at wavelength λ can be expressed as $d(\sin\theta_{i_1} \pm \sin\theta_{d1}) = j\lambda = d(\sin\theta_{i_2} \pm \sin\theta_{d2})$. Then, a difference equation about diffraction angles and incident angles is obtained, which can be expressed: $\sin\theta_{i_1} - \sin\theta_{i_2} = \pm(\sin\theta_{d2} - \sin\theta_{d1})$. Base on the precondition that re-imaging 1st lens and re-imaging 2nd lens have the same focal length f, both sides of the previous difference equation multiply f. And then it is turned into $f(\sin\theta_{i_1} - \sin\theta_{i_2}) = \pm f(\sin\theta_{d2} - \sin\theta_{d1})$. As we know, $f\sin\theta_{d1}$ is the dispersing distance of wavelength λ on the image sensor. Right side of the equation is the distance of the two pixels at wavelength λ on dispersed image. Left side is distance of the two pixels on non-dispersed image. So the feature shift invariability shown in Fig. 2 is demonstrated. Base on the shift invariability, an equation (Eq. (2)) to describe relation between light intensity on CCD 1st and CCD 2nd is obtained. Specifically, this relation can be expressed as that the dispersed image on CCD 2nd $f(x)$ equals the convolution between non-dispersed image observed on CCD 1st $\varphi(x)$ and the spectral of source.

$$f(x) = \varphi(x) * S(x;\lambda), \tag{2}$$

where $f(x)$ is dispersed image observed on CCD 2nd; $\varphi(x)$ is non-dispersed image observed on CCD 1st; $*$ denotes the convolution; $S(x;\lambda)$ is the spectral function which can be acquired by solving inverse problem deconvolution of $f(x)$ and $\varphi(x)$.

In this experiment, a 200-μm wide slit is used to acquire overlapped data and a 5-μm wide slit is used to obtain standard spectrum to evaluate accuracy of reconstructed spectrum. 5-μm wide slit is chosen, because the pixel of CCD is about 5-μm too. Smaller slit would not improve the spectral resolution. All lenses except objective lens are the same CCTV lens (FL: 25 mm, f-number: 1.4), which has a better aberration correction and makes the system easily assembled. A plane beam splitter (30% reflection, 70% transmission; BSS16 ThorLab, USA) is employed to construct two function-different optical paths. A bladed grating with 300 grooves/mm groove intensity (blade angle: 4°18′; GR50-0305, ThorLab, USA) is used as dispersing component. The two image sensors are the same industrial camera with 1280×1024 resolution (pixel width: 5.2 μm; DH-HV1351UM Daheng, China).

The first light source used is a deuterium lamp, which is placed 50 cm in front of the objective lens. In order to quantify the proposed method high-throughput advantage, a filter is utilized to weaken the deuterium. The direction of dispersing is only along x-axis, pixels along y-axis have the same spectrum distribution, and they can be treated as one pixel. So, pixels in the same column are summed as one pixel to turn an image into a curve. Data pre-processing is described in Fig. 3.

The measured non-dispersed and dispersed light intensity are shown in Fig. 4, with background noise removed. The blue curve is light intensity of non-dispersed and red curve is spectrum-overlapped from different pixels along x-axis.

However, deconvolution belongs to the class of so-called ill-posed problems. Both observation and convolution

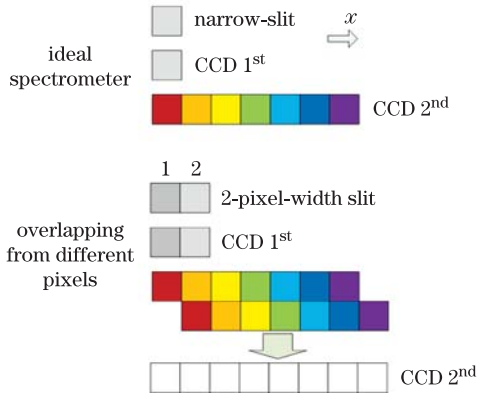

Fig. 2. (Color online) Demonstration of double shifting caused by different pixels and wavelengths.

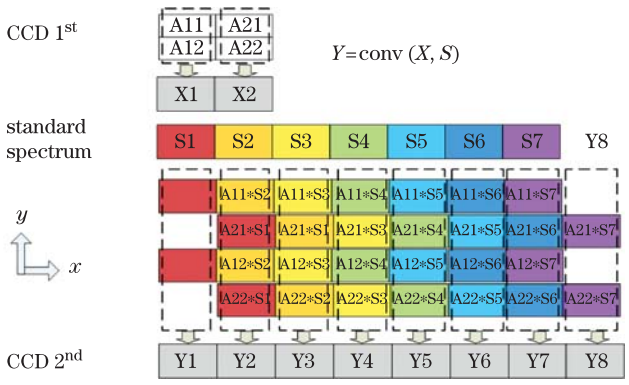

Fig. 3. (Color online) Flow of data pre-processing.

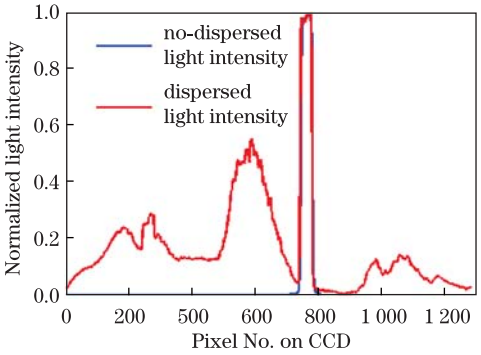

Fig. 4. (Color online) Measured light intensity of both non-dispersed and dispersed for deuterium lamp.

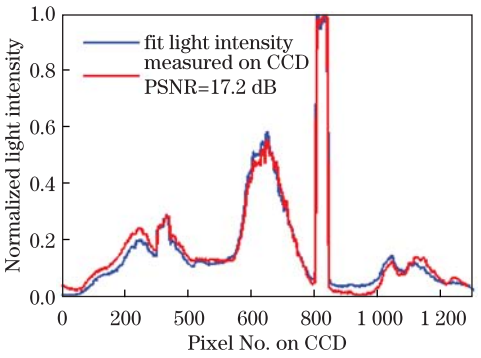

Fig. 5. (Color online) Dispersed light intensity of 200-μm slit both measured and fit for deuterium lamp.

kernel are not acquired precisely every measurement, so the noise is inevitable. And even worse, small noise may cause large perturbation in the solution of deconvolution. Moreover, the response of the CCD is not very linear, and it causes distinct difference between measured and fit light intensity of 200-μm slit. This unexpected error of CCD is shown in Fig. 7. Accurately, pixels is a little oversaturation while measuring the peak of red curve in Fig. 5, the measured value is a little smaller than the real light intensity.

As a mathematic problem, deconvolution is well developed and several great solutions are proposed to deal with this problem, such as Richardson-Lucy deconvolution[10], which is employed to reconstruct spectrum in Ref. [11]. In Fig. 5, two similar curves can be seen. The blue one is the convolution result between measured spectrum with a 5-μm slit and non-dispersed light intensity with a 200-μm slit (blue curve in Fig. 4). The red one is measured dispersing data with a 200-μm slit which already has shown in Fig. 4 (red curve). As a matter of fact, the observation (red curve in Fig. 5) does not fit the ideal data perfectly due to non-linear response of CCD.

Figure 6 shows both the reconstructed spectrum data (blue) and measured spectrum with a 5-μm slit (red). We can see that two characteristic spectrum of deuterium lamp are significantly recovered and the reconstructed spectrum fitted the standard spectrum well, except that there are a few periodic perturbations in the restored data. The unexpected perturbation is caused by several reasons: image aberration, non-linear response of CCD, and noise (introduced by ill-pose of deconvolution). Due to high-throughput, the peak signal-to-noise ratio (PSNR)=15.2 dB of proposed method is much higher than traditional spectrometer (PSNR=9.8 dB). And the measured spectrum with 200-μm slit exhibits about 17.2 dB, if the fitted curve (blue curve in Fig. 5) is regard as standard spectrum of 200-μm-slit.

Another light source we used is LED with two types of LED combined. The measured and fitted light intensity of 200 μm slit are showed in Fig. 8, the PSNR of measured light intensity is 24.8 dB. It is much smoother without many weak peaks compared to the spectrum of the first light source. Due to the smooth of LED's spectrum, the reconstructed data (Fig. 9) matches standard data very well. Moreover, there is about 6-dB improvement contributed by the proposed method (PSNR=24.1 dB) compared with traditional spectrometer (PSNR=18.4 dB).

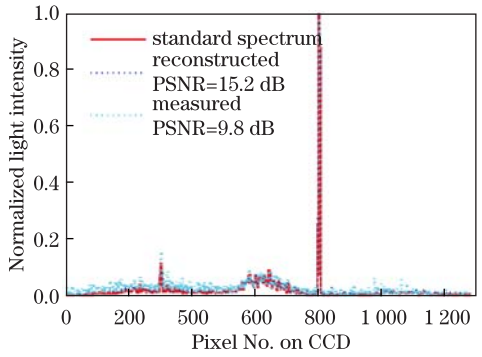

Fig. 6. (Color online) Results of reconstructed spectrum and measured spectrum with 5-μm slit for deuterium lamp.

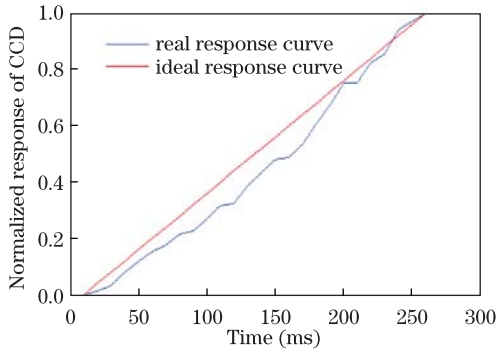

Fig. 7. (Color online) Demonstration of non-linear response of CCD.

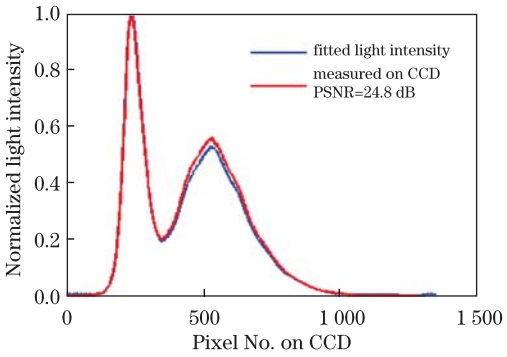

Fig. 8. (Color online) Dispersed light intensity of 200-μm slit both measured and fit for two combined LEDs.

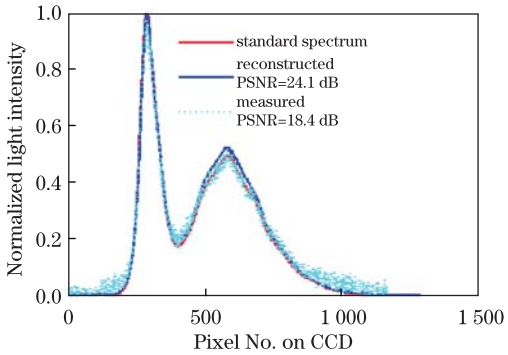

Fig. 9. (Color online) Results of reconstructed spectrum and measured spectrum with 5-μm slit for two combined LEDs.

In conclusion, using a beam splitter to construct two function-different light paths, both non-dispersed and dispersed light intensity can be measured. Based on shift invariability, the spectrum of light source is reconstructed by solving the deconvolution problem. This new design of spectrometer can achieve a high resolution and remain high-throughput without any spatial modulation. This method is an effective realization to improve the performance of traditional spectrometer, especially the light source tends to be weak. We are currently working on obtaining more reliable and accurate spectrum by decreasing errors from the system and reconstruction algorithm, such as finding a better linear response CCD and analyzing the errors associated with deconvolution procedures.

This work was supported by the National Natural Science Foundation of China (No. 61231014). The authors would like to thank the anonymous viewers whose numerous suggestions helped to improve the quality of this letter.

References

1. P. Jacquinot, Rep. Prog. Phys. **23,** 267 (1960).
2. E. C. Cull, M. E. Gehm, D. J. Brady, C. R. Hsieh, O. Momtahan, and A. Adibi, Appl. Opt. **46,** 365 (2007).
3. J. A. Decker, Appl. Opt. **10,** 510 (1971).
4. P. Hansen and J. Strong, Appl. Opt. **11,** 502 (1972).
5. M. E. Gehm, S. T. McCain, N. P. Pitsianis, D. J. Brady, P. Potuluri, and M. E. Sullivan, Appl. Opt. **45,** 2965 (2006).
6. D. Kittle, K. Choi, A. Wagadarikar, and D. J. Brady, Appl. Opt. **49,** 6824 (2010).
7. C. Y. Huang and W. C. Wang, Opt. Lett. **37,** 1559 (2012).
8. J. Chen, Y. Zhu, B. Liu, W. Wei, N. Wang, and J. Zhang, Chin. Opt. Lett. **11,** 053003 (2013).
9. Q. Yang, B. Zhao, and X. Zeng, Chin. Opt. Lett. **11,** 021202 (2013).
10. L. B. Lucy, Astron. J. **79,** 745 (1974).
11. M. A. Golub, M. Nathan, A. Averbuch, E. Lavi, V. A. Zheludev, and A. Schclar, Appl. Opt. **48,** 1520 (2009).